INTERNATIONAL JOURNAL FOR NUMERICAL AND ANALYTICAL METHODS IN GEOMECHANICS, VOL. 21, 379–395 (1997)

SURFACE DISPLACEMENTS OF A NON-HOMOGENEOUS ELASTIC HALF-SPACE SUBJECTED TO UNIFORM SURFACE TRACTIONS. PART II: LOADING ON RECTANGULAR SHAPED AREAS

R. F. STARK* AND J. R. BOOKER

School of Civil and Mining Engineering, University of Sydney, N.S.W. 2006, Australia

SUMMARY

An alternative approach for calculating the surface displacements of a non-homogeneous half-space acted upon by a vertical and/or horizontal load, uniformly distributed over a rectangular area, is presented in this part of the paper. The procedure proposed proves to be extremely efficient since the displacements can be found without numerical integration for this special loading pattern. Comparisons with solutions for rectangular loaded areas on Boussinesq- and Gibson-type soil show perfect agreement. In the case of the non-homogeneous half-space the procedure was checked using the method outlined in the first part of this paper revealing that both approaches come up with identical answers. Some results of a parametric study are presented for the surface displacements of a non-homogeneous half-space subject to vertical and horizontal loading. In this study both the material properties of the soil mass, i.e. Young's modulus and Poisson's ratio and the aspect ratio of the loading are varied. These results are presented in the form of influence charts which may readily be used in hand calculations for estimating the displacements of footings on a non-homogeneous soil. © 1997 by John Wiley & Sons, Ltd.

Int. J. Numer. Anal. Meth. Geomech., Vol. 21, 379–395 (1997)
(No. of Figures: 7 No. of Tables: 2 No. of Refs: 15)

Key words: elastic half-space; homogeneous; non-homogeneous; integration free approach; surface displacement; rectangular shaped loading area

1. INTRODUCTION

In the first part of this paper a numerical scheme was presented enabling the calculation of surface displacements of a non-homogeneous soil base subjected to any combination of vertical and horizontal loading uniformly distributed over an arbitrarily shaped area. Thus, at first glance, it might not be obvious why investigation of the issue of the rectangular shaped load pattern is undertaken in further detail. However, since footings and foundation structures very often tend to be of a rectangular shape in plan, this kind of load pattern plays a predominant role in foundation

*Correspondence to: R. F. Stark, Institute for Strength of Materials, University of Innsbruck, Technikerstr. 13, A-6020 Innsbruck, Austria

Contract grant sponsor: Austrian Science Foundation; contract grant number: J0963-Tec

CCC 0363–9061/97/060379–17$17.50

Received 17 March 1995
Revised 27 August 1996

engineering and therefore any achievable improvement of the numerical procedure for this special load case is of direct practical interest.

The fact mentioned above has been recognized long ago and is reflected by numerous works in the field of geotechnical literature. Of course, the early works dealt with a homogeneous mass. Schleicher[1] seems to have been one of the first to publish a solution for the surface settlement of the homogeneous half-space underneath the corner of a rectangle subjected to a uniform vertical loading. Steinbrenner[2] presented influence charts to calculate vertical displacements at any point within the homogeneous soil mass under the corner of the loaded rectangle. Tölke[3] worked out formulas to determine the displacement components (u_x, u_y, u_z) of any arbitrary point (x, y, z) of the homogeneous half-space, loaded by a constant traction (p_x, p_y, p_z) uniformly distributed over a rectangular area. Explicit formulas, tables and charts can be found in many related text books such as Harr,[4] Kany[5] and in Giroud,[6] perhaps one of the most comprehensive works.

Besides, several attempts were made to model the soil mass as a non-homogeneous medium, since in nature the rigidity of the soil is very likely to increase with depth in many cases due to the overburden pressure. Brown and Gibson[7] studied the case of an isotropic linearly non-homogeneous half-space subject to loading normal to its plane boundary applied on a rectangular area and published influence charts for the corner settlement.

In foundation engineering practice the finite element method has nowadays become a standard tool for analysing raft foundations. It is common sense that rectangular shaped finite elements tend to give most accurate results and therefore are used whenever possible. Beyond that, footings and foundation rafts are very often rectangular in plane, and therefore it is likely that in many cases the finite element mesh will at least partially be made of rectangular elements. In a soil–structure interaction analysis of this type it is usually assumed that the contact stresses acting in the soil–structure interface may be approximated using a constant stress distribution within a single element, provided that an adequate discretization of the raft was done. Hence, very often we are faced with the instance that uniform tractions are acting on rectangular shaped elements. It therefore seems reasonable to draw special attention to this form of loading pattern in order to increase the efficiency of the numerical procedure. As will be shown, it is possible to find the surface displacements of both homogeneous and non-homogeneous half-space without numerical integration if the traction is acting on a rectangular shaped area.

2. MATHEMATICAL DERIVATION

In this section the mathematical formulas required to compute the displacement components of any point $(x, y, 0)$ of the surface of a non-homogeneous half-space which is acted upon by a uniformly distributed load on a rectangular area are developed. The non-homogeneity considered is a variation in Young's modulus E with depth z below the surface, i.e.

$$E(z) = m_E z^{\alpha} \quad 0 \leqslant \alpha \leqslant 1 \tag{1}$$

whereas Poisson's ratio is assumed to be constant. As shown in Figure 1, a right handed co-ordinate system is adopted where the xy-plane is attached to the surface of the half-space and the positive z-axis measures the depth underneath the surface of the half-space. This is consistent with the usual convention in soil mechanics, taking compressive stresses and strains as positive quantities.

Based on the results found by Booker *et al.*[8] the displacement at a point $(x, y, 0)$ of the non-homogeneous half-space can be expressed by the following matrix equation

$$\mathbf{u} = \mathbf{\Lambda p} \tag{2}$$

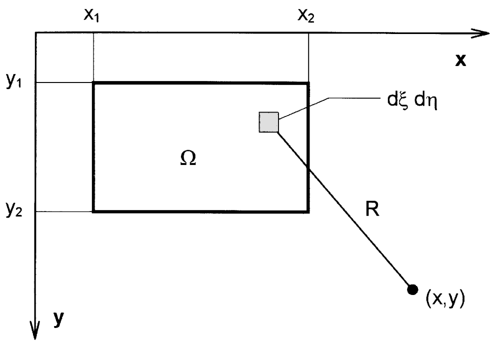

Figure 1. Uniformly distributed load over a rectangular area

where

$$\mathbf{u} = (u_x, u_y, u_z)^{\mathrm{T}}$$
$$\mathbf{p} = (p_x, p_y, p_z)^{\mathrm{T}} \tag{3}$$

u denotes the surface displacement vector, **p** the vector of the external surface tractions which are assumed to be uniformly distributed over the rectangular area Ω and the matrix $\mathbf{\Lambda}$ is given by

$$\mathbf{\Lambda} = \frac{1}{m_E} \int\int_{\Omega} \mathbf{\Psi}\, \mathrm{d}\xi\, \mathrm{d}\eta \tag{4}$$

where $\mathbf{\Psi}$ takes the form

$$\mathbf{\Psi} = \begin{bmatrix} \frac{(H+K)}{2}\psi_4 + \frac{(H-K)}{2}\psi_5 & (H-K)\psi_6 & A\psi_2 \\ (H-K)\psi_6 & \frac{(H+K)}{2}\psi_4 - \frac{(H-K)}{2}\psi_5 & A\psi_3 \\ L\psi_2 & L\psi_3 & B\psi_1 \end{bmatrix} \tag{5}$$

The coefficients A, B, H, K, L and the functions ψ_i with its associated terms γ_i, $i = 1, 2, \ldots, 6$, have already been defined in the first part of this paper and the geometric relation between load point and field point is given by

$$R = \sqrt{u^2 + v^2}$$
$$u = x - \xi \tag{6}$$
$$v = y - \eta$$

As indicated by (5) the displacement vector of a specific point of the surface of the non-homogeneous half-space is related to six different functions ψ_i. These six cases will be examined hereafter separately.

Case 1: For the time being, let us focus our attention on the simplest case, i.e. when the displacement in z direction caused by a uniform load acting in the same direction is sought. In this instance we have

$$\psi_1 = R^{\gamma_1} \tag{7}$$

and the displacement component u_{zz} is given by

$$u_{zz} = \frac{Bp_z}{m_E} \int_{y_1}^{y_2} \int_{x_1}^{x_2} R^{\gamma_1} \, d\xi \, d\eta = \frac{Bp_z}{m_E} \lambda_1 \tag{8}$$

This particular case has been investigated by Booker.[9] Using equation (6) the above double integral can be rewritten

$$\lambda_1(x, y) = \int_{y-y_2}^{y-y_1} \int_{x-x_2}^{x-x_1} \psi_1 \, du \, dv \tag{9}$$

where $x_1 < x_2$ and $y_1 < y_2$ as depicted in Figure 1.

Let us now drop the subscripts for a moment for the sake of generality and suppose we can find a function κ so that

$$\frac{\partial^2 \kappa}{\partial u \partial v} = \psi(u, v) \tag{10}$$

where ψ is a homogeneous function, then

$$\lambda(x, y) = \kappa(x - x_1, y - y_1) - \kappa(x - x_1, y - y_2) + \kappa(x - x_2, y - y_2) - \kappa(x - x_2, y - y_1). \tag{11}$$

Since the integral in (8) can always be split up with respect to its boundaries, it is sufficient to deal with

$$\kappa(\gamma) = \int_0^v \int_0^u \psi(\gamma) \, d\bar{u} \, d\bar{v} \tag{12}$$

where the notation $\bar{u}$ and $\bar{v}$ are simply used to distinguish between the integral boundaries and the integration variables. As expressed by (12), κ represents the double integral of ψ, which itself is a homogeneous function of order γ. Hence, κ must be a homogeneous function of order $\gamma + 2$.

Substituting the first derivatives of κ with respect to u and v by F and G, respectively, i.e.

$$\begin{aligned} \frac{\partial \kappa}{\partial v} &= \int_0^u \psi(\gamma) \, d\bar{u} = F(\gamma) \\ \frac{\partial \kappa}{\partial u} &= \int_0^v \psi(\gamma) \, d\bar{v} = G(\gamma) \end{aligned} \tag{13}$$

and making use of Euler's theorem, κ can be expressed by the following relationship

$$\kappa(\gamma) = \frac{vF(\gamma) + uG(\gamma)}{\gamma + 2} \tag{14}$$

In the case of u_{zz}, where $\psi = \psi_1$, κ_1 simply becomes

$$\kappa_1 = \frac{vF(\gamma_1) + uG(\gamma_1)}{\gamma_1 + 2} \tag{15}$$

where

$$\begin{aligned} F(\gamma_1) &= \int_0^u R^{\gamma_1} \, d\bar{u} = \frac{\operatorname{sgn}(u)|v|^{(\gamma_1+1)}}{2} B_\zeta(a, b) \\ G(\gamma_1) &= \int_0^v R^{\gamma_1} \, d\bar{v} = \frac{\operatorname{sgn}(v)|u|^{(\gamma_1+1)}}{2} B_{(1-\zeta)}(a, b) \end{aligned} \tag{16}$$

and $B_\zeta(a, b)$ is the incomplete Beta function, its parameters given by

$$\zeta = \frac{u^2}{u^2 + v^2}$$

$$a = \frac{1}{2} \tag{17}$$

$$b = \frac{-(\gamma_1 + 1)}{2}$$

As shown, for a rectangular loaded area the displacement u_{zz} can be found without performing any numerical integration at all, since the double integral represented by λ_1 of equation (8) can be substituted by the evaluation of the function κ_1 at four distinct locations according to (11).

Case 2: In this instance ψ_2 is given by

$$\psi_2 = uR^{\gamma_2} \tag{18}$$

From partial differentiation of (7) with respect to u and by setting $\gamma_1 = \gamma_2 + 2$ we find

$$\psi_2 = \frac{1}{\gamma_2 + 2} \frac{\partial \psi_1(\gamma_2 + 2)}{\partial u} \tag{19}$$

Hence, κ_2 can be derived from κ_1, i.e.

$$\kappa_2 = \frac{1}{\gamma_2 + 2} \frac{\partial \kappa_1(\gamma_2 + 2)}{\partial u} \tag{20}$$

and so the function κ_2 which satisfies condition (10) takes the form

$$\kappa_2 = \frac{u^2 G(\gamma_2)}{(\gamma_2 + 4)} + \frac{G(\gamma_2 + 2) + vR^{(\gamma_2 + 2)}}{(\gamma_2 + 2)(\gamma_2 + 4)} \tag{21}$$

Case 3: In this case, where ψ_3 is given by

$$\psi_3 = vR^{\gamma_3} \tag{22}$$

κ_3 can be derived from Case 2 simply by interchanging the variables and we get

$$\kappa_3 = \frac{v^2 F(\gamma_3)}{(\gamma_3 + 4)} + \frac{F(\gamma_3 + 2) + uR^{(\gamma_3 + 2)}}{(\gamma_3 + 2)(\gamma_3 + 4)} \tag{23}$$

Case 4: Here ψ_4 is given by

$$\psi_4 = (u^2 + v^2) R^{\gamma_4} = R^{(\gamma_4 + 2)} \tag{24}$$

which would be identical with Case 1 if we set $\gamma_1 = \gamma_4 + 2$. Hence, the solution then is

$$\kappa_4 = \frac{vF(\gamma_4 + 2) + uG(\gamma_4 + 2)}{\gamma_4 + 4} \tag{25}$$

Case 5: For this instance the function ψ_5 is given by

$$\psi_5 = (u^2 - v^2) R^{\gamma_5} \tag{26}$$

Using the second partial derivatives of (7) with respect to u and v are and setting $\gamma_1 = \gamma_5 + 4$, ψ_5 can be expressed by ψ_1, i.e.

$$\psi_5 = \frac{1}{(\gamma_5 + 4)(\gamma_5 + 2)} \left[\frac{\partial^2 \psi_1(\gamma_5 + 4)}{\partial u^2} - \frac{\partial^2 \psi_1(\gamma_5 + 4)}{\partial v^2} \right] \tag{27}$$

and therefore κ_5 is found from κ_1, and is given by

$$\kappa_5 = \frac{u^3 G(\gamma_5) - v^3 F(\gamma_5)}{\gamma_5 + 6} + \frac{3[uG(\gamma_5 + 2) - vF(\gamma_5 + 2)]}{(\gamma_5 + 2)(\gamma_5 + 6)} \tag{28}$$

Case 6: Here ψ_6 is given by

$$\psi_6 = uvR^{\gamma_6} \tag{29}$$

From partial differentiation of ψ_1 with respect to u and v it follows that ψ_6 and κ_6 can be constructed from ψ_1 and κ_1, respectively, namely

$$\psi_6 = \frac{1}{(\gamma_6 + 4)(\gamma_6 + 2)} \frac{\partial^2 \psi_1(\gamma_6 + 4)}{\partial u \partial v} \tag{30}$$

and

$$\kappa_6 = \frac{1}{(\gamma_6 + 4)(\gamma_6 + 2)} \frac{\partial^2 \kappa_1(\gamma_6 + 4)}{\partial u \partial v} \tag{31}$$

Again using the partial derivatives of (13) with respect to u and v and with the appropriate substitutions by ψ_6 the solution for κ_6 is found to be

$$\kappa_6 = \frac{R^{(\gamma_6 + 4)}}{(\gamma_6 + 4)(\gamma_6 + 2)} \tag{32}$$

With the solutions for κ_i, $i = 1, 2, \ldots, 6$ at hand, the matrix $\mathbf{\Lambda}$ can now easily be established by means of equation (11) i.e.

$$\mathbf{\Lambda} = \begin{bmatrix} \frac{(H+K)}{2}\lambda_4 + \frac{(H-K)}{2}\lambda_5 & (H-K)\lambda_6 & A\lambda_2 \\ (H-K)\lambda_6 & \frac{(H+K)}{2}\lambda_4 - \frac{(H+K)}{2}\lambda_5 & A\lambda_3 \\ L\lambda_2 & L\lambda_3 & B\lambda_1 \end{bmatrix} \tag{33}$$

and finally the displacement of any point of the surface of the non-homogeneous half-space subject to a constant surface traction within a rectangular area can be evaluated using equation (2).

It is noteworthy to point out that, analogous to the case of the homogeneous half-space, the method proposed enables computation of the surface displacements due to any kind of uniformly distributed surface load acting on a rectangular area of the non-homogeneous half-space without numerical integration. Hence, with regard to the numerical analysis both homogeneous and non-homogeneous half-space can be analysed very efficiently using a single numerical scheme.

3. NUMERICAL RESULTS

For a first check a homogeneous half-space and a Gibson soil were considered and the results obtained with the method proposed were compared with well-known solutions published by

Poulos and Davis.[10] These comparisons showed perfect agreement for all displacement components due to vertical and horizontal loading on the rectangle. However, these checks were restricted to the two limiting cases of non-homogeneity described by equation (1). For a more comprehensive examination of the method and its numerical implementation into a FORTRAN code, the procedure outlined in the first part of this paper was used. This investigation revealed that both methods yield the same results for any degree of non-homogeneity. Of course, since there is no numerical integration required in this approach, this procedure is much more efficient and the results depend neither on the discretization scheme nor on the applied quadrature rule.

3.1. Surface displacements of a uniformly loaded strip

A further means to check the proposed method is to use the solutions for a uniformly loaded strip on an non-homogeneous half-space. In fact, the displacement components at the middle of the longer side of a rectangle with length L and width B should converge to the displacements at the edge of a strip of the same width, i.e. $2c = B$ when the aspect ratio L/B of the rectangle tends to infinity. Consistent with the orientation of the rectangle adopted in the next section, it is assumed that the longitudinal direction of the strip runs parallel to the x-axis, in order to facilitate direct comparison of the individual displacement components between strip and rectangle.

Using the solution given by Booker *et al.*[8,11] the surface displacements $\mathbf{u}$ for a uniformly distributed traction $\mathbf{p}$ acting over the strip $-c \leqslant y \leqslant c$ is given by

$$\begin{Bmatrix} u_x \\ u_y \\ u_z \end{Bmatrix} = \frac{\operatorname{sgn}(y+c)|y+c|^{1-\alpha} - \operatorname{sgn}(y-c)|y-c|^{1-\alpha}}{m_E(1-\alpha)} \begin{bmatrix} k & 0 & 0 \\ 0 & h & a\operatorname{sgn}(y) \\ 0 & l\operatorname{sgn}(y) & b \end{bmatrix} \begin{Bmatrix} p_x \\ p_y \\ p_z \end{Bmatrix} \tag{34}$$

where the coefficients a, b, h, k and l were already defined in the first part of this paper.

In contrast to the results for the homogeneous half-space and the Gibson-type soil all displacement components remain finite for a non-homogeneous half-space of the type $0 < \alpha < 1$, which is in agreement with the physical reality of the problem. However, since both limiting cases might be of interest to check the method proposed, these results have been summarized in Table I.

For the case of a non-homogeneous half-space equation (34) has been evaluated for the edge of the strip and the results are given in Table II in the form of influence factors IS_{rs}. With these influence factors, the surface displacements u_{rs} at the edge of the strip may readily be calculated using the following expression:

$$u_{rs} = \frac{p_s(2c)^{(1-\alpha)}}{m_E} IS_{rs} \tag{35}$$

where r is the displacement direction and s the direction in which the loading p is acting on the strip. For completeness it should be mentioned that

$$u_{yz}|_{y=+c} = -u_{yz}|_{y=-c} \tag{36}$$

which is not reflected in (35) but follows from symmetry and is also indicated by (34). It might be interesting to notice that the horizontal displacements due to vertical loading are directed away from the loaded area for those combinations of Poisson's ratio and non-homogeneity parameter which lead to a negative coefficient a, as can be seen from Table II.

The edge displacements of the strip, summarized in Tables I and II, may be compared with the corresponding surface displacements at the corner of a rectangle whose aspect ratio tends to

Table I. Surface displacement field for a uniformly loaded strip

		$\alpha = 0$		$0 < \alpha < 1$	$\alpha = 1$	
		$0 \leqslant v < 0{\cdot}5$	$v = 0{\cdot}5$	$0 \leqslant v \leqslant 0{\cdot}5$	$0 \leqslant v < 0{\cdot}5$	$v = 0{\cdot}5$
u_{xx}	$\lvert y\rvert \leqslant c$	∞	∞	Equation (34)	∞	∞
u_{xx}	$\lvert y\rvert > c$	∞	∞	Equation (34)	$\dfrac{-p_x(v+1)}{m_E}[\log(\lvert y\rvert - c) - \log(\lvert y\rvert + c)]$	$\dfrac{-3p_x}{2m_E}[\log(\lvert y\rvert - c) - \log(\lvert y\rvert + c)]$
u_{yy}	$\lvert y\rvert \leqslant c$	∞	∞	Equation (34)	∞	∞
u_{yy}	$\lvert y\rvert > c$	∞	∞	Equation (34)	$\dfrac{4p_y(v^2-1)}{m_E\pi}[\log(\lvert y\rvert - c) - \log(\lvert y\rvert + c)]$ $\sin\left(\pi\sqrt{\dfrac{(2v-1)}{2(v-1)}}\right)\sqrt{\dfrac{(v-1)}{2(2v-1)}}$	$\dfrac{-3p_y}{2m_E}[\log(\lvert y\rvert - c) - \log(\lvert y\rvert + c)]$
u_{yz}	$\lvert y\rvert \leqslant c$	$c(2v-1)(v+1)$ $\operatorname{sgn}(y)$	0	Equation (34)	∞	∞
u_{yz}	$\lvert y\rvert > c$	$c(2v-1)(v+1)$ $\operatorname{sgn}(y)$	0	Equation (34)	$\dfrac{2p_z(v^2-1)}{m_E\pi}[\log(\lvert y\rvert - c) - \log(\lvert y\rvert + c)$ $\cos\left(\pi\sqrt{\dfrac{(2v-1)}{2(v-1)}}\right)\operatorname{sgn}(y)$	$\dfrac{-3p_z}{2m_E\pi}[\log(\lvert y\rvert - c) - \log(\lvert y\rvert + c)]\operatorname{sgn}(y)$
u_{zz}	$\lvert y\rvert < c$	∞	∞	Equation (34)	∞	$\dfrac{3p_z}{2m_E}$
u_{zz}	$\lvert y\rvert = c$	∞	∞	Equation (34)	∞	$\dfrac{3p_z}{4m_E}$
u_{zz}	$\lvert y\rvert > c$	∞	∞	Equation (34)	$\dfrac{p_z(v^2-1)}{m_E\pi}[\log(\lvert y\rvert - c) - \log(\lvert y\rvert + c)]$ $\sin\left(\pi\sqrt{\dfrac{(2v-1)}{2(v-1)}}\right)$	0

Table II. Influence factors for the surface displacements of a non-homogeneous half-space at the edge of a strip, subject to uniform vertical or horizontal loading

	α	$v = 0{\cdot}0$	$v = 0{\cdot}1$	$v = 0{\cdot}2$	$v = 0{\cdot}3$	$v = 0{\cdot}4$	$v = 0{\cdot}5$
	0·1	7·55224E + 0	8·30746E + 0	9·06269E + 0	9·81791E + 0	1·05731E + 1	1·13284E + 1
	0·2	4·50531E + 0	4·95584E + 0	5·40638E + 0	5·85691E + 0	6·30744E + 0	6·75797E + 0
	0·3	3·62035E + 0	3·98239E + 0	4·34442E + 0	4·70646E + 0	5·06849E + 0	5·43053E + 0
	0·4	3·32562E + 0	3·65819E + 0	3·99075E + 0	4·32331E + 0	4·65587E + 0	4·98844E + 0
u_{xx}	0·5	3·33851E + 0	3·67236E + 0	4·00621E + 0	4·34006E + 0	4·67391E + 0	5·00776E + 0
	0·6	3·62431E + 0	3·98674E + 0	4·34917E + 0	4·71160E + 0	5·07403E + 0	5·43647E + 0
	0·7	4·30421E + 0	4·73463E + 0	5·16505E + 0	5·59548E + 0	6·02590E + 0	6·45632E + 0
	0·8	5·85546E + 0	6·44101E + 0	7·02655E + 0	7·61210E + 0	8·19764E + 0	8·78319E + 0
	0·9	1·07654E + 1	1·18420E + 1	1·29185E + 1	1·39950E + 1	1·50716E + 1	1·61481E + 1
	0·1	7·72086E + 0	7·66908E + 0	7·46745E + 0	7·11594E + 0	6·61447E + 0	5·96295E + 0
	0·2	4·68264E + 0	4·67221E + 0	4·57461E + 0	4·38972E + 0	4·11740E + 0	3·75735E + 0
	0·3	3·80566E + 0	3·81936E + 0	3·76607E + 0	3·64561E + 0	3·45766E + 0	3·20167E + 0
	0·4	3·51826E + 0	3·55676E + 0	3·53782E + 0	3·46112E + 0	3·32613E + 0	3·13195E + 0
u_{yy}	0·5	3·53786E + 0	3·60862E + 0	3·62719E + 0	3·59306E + 0	3·50543E + 0	3·36294E + 0
	0·6	3·82981E + 0	3·94850E + 0	4·01805E + 0	4·03774E + 0	4·00642E + 0	3·92210E + 0
	0·7	4·51533E + 0	4·71474E + 0	4·86680E + 0	4·97048E + 0	5·02418E + 0	5·02521E + 0
	0·8	6·07171E + 0	6·43488E + 0	6·75162E + 0	7·02058E + 0	7·23959E + 0	7·40507E + 0
	0·9	1·09863E + 1	1·18464E + 1	1·26604E + 1	1·34265E + 1	1·41420E + 1	1·48020E + 1
	0·1	− 5·65510E − 1	− 4·91501E − 1	− 3·93726E − 1	− 2·72165E − 1	− 1·26786E − 1	4·24693E − 2
	0·2	− 6·45720E − 1	− 5·54376E − 1	− 4·34536E − 1	− 2·86095E − 1	− 1·08885E − 1	9·73960E − 2
	0·3	− 7·47049E − 1	− 6·33693E − 1	− 4·85702E − 1	− 3·02773E − 1	− 8·44046E − 2	1·70280E − 1
	0·4	− 8·80186E − 1	− 7·37876E − 1	− 5·52645E − 1	− 3·23773E − 1	− 5·00934E − 2	2·70429E − 1
u_{yz}	0·5	− 1·06436E + 0	− 8·82073E − 1	− 6·45077E − 1	− 3·51866E − 1	1·43093E − 16	4·14743E − 1
	0·6	− 1·33804E + 0	− 1·09655E + 0	− 7·82377E − 1	− 3·92515E − 1	7·78891E − 2	6·37184E − 1
	0·7	− 1·79094E + 0	− 1·45189E + 0	− 1·00971E + 0	− 4·58387E − 1	2·11735E − 1	1·01719E + 0
	0·8	− 2·69219E + 0	− 2·15980E + 0	− 1·46249E + 0	− 5·87361E − 1	4·86192E − 1	1·79336E + 0
	0·9	− 5·38748E + 0	− 4·27880E + 0	− 2·81766E + 0	− 9·68634E − 1	1·32485E + 0	4·15923E + 0
	0·1	7·01897E + 0	6·89443E + 0	6·61888E + 0	6·19179E + 0	5·61228E + 0	4·87878E + 0
	0·2	3·90220E + 0	3·80699E + 0	3·62156E + 0	3·34455E + 0	2·97368E + 0	2·50490E + 0
	0·3	2·92743E + 0	2·84004E + 0	2·67971E + 0	2·44376E + 0	2·12779E + 0	1·72397E + 0
	0·4	2·51304E + 0	2·42763E + 0	2·27432E + 0	2·04842E + 0	1·74226E + 0	1·34226E + 0
u_{zz}	0·5	2·35857E + 0	2·27209E + 0	2·11586E + 0	1·88208E + 0	1·55797E + 0	1·12098E + 0
	0·6	2·39363E + 0	2·30329E + 0	2·13459E + 0	1·87467E + 0	1·50241E + 0	9·80526E − 1
	0·7	2·65608E + 0	2·55767E + 0	2·36183E + 0	2·04667E + 0	1·57621E + 0	8·86802E − 1
	0·8	3·37317E + 0	3·25716E + 0	3·00072E + 0	2·56307E + 0	1·87693E + 0	8·22785E − 1
	0·9	5·78228E + 0	5·61147E + 0	5·16412E + 0	4·34091E + 0	2·97726E + 0	7·79055E − 1

infinity using the charts in Figures 2, and 5–7. Due to symmetry the displacement at the corner of the rectangle should be half the corresponding strip displacement. The results of this comparison confirmed the correctness of the method proposed.

3.2. Uniform traction on a rectangular area

In practice of shallow foundation engineering, the loaded area very often happens to be of rectangular shape or in many cases at least it can be approximated by such. Therefore, this load pattern is of particular interest and there exist a great variety of elastic solutions for distributed loadings on the surface of a semi-infinite mass.[10,12] For hand calculation of the surface settlement of the homogeneous half-space subjected to a uniformly distributed vertical load on a rectangle for instance, the well-known charts of Steinbrenner[2] or Giroud[13] may be used. In this section analogous charts for the non-homogeneous half-space described by equation (1) which may be acted upon by vertical and horizontal loading are provided. The whole range of non-homogeneity was investigated in this study and charts have been drawn up for several degrees of non-homogeneity from $\alpha = 0$ to $\alpha = 0.9$ in steps of 0·1 and different Poisson's ratios. However, only some of these are reproduced in this section. For full detail see Reference.[14]

The charts in Figures 2–7 show influence factors I_{rs} for a certain displacement component u_{rs} at the corner of a rectangle for non-homogeneity parameters 0, 0·5 and 0·9 and Poisson's ratios between 0 and 0·5. For easier use the kind of loading and the displacement component under consideration are depicted in a small figure in each chart. It should be mentioned that these results are valid for the corner of the rectangle lying at the origin of the co-ordinate system. For other locations the sign of the displacement component might have to be changed as indicated in the figures of the charts.

The relation between the influence factor I_{rs} and the surface displacement u_{rs}, i.e. the displacement in direction r caused by a uniformly distributed load p_s on the rectangle acting in direction s, is given by

$$u_{rs} = \frac{p_s B^{(1-\alpha)}}{m_E} I_{rs} \tag{37}$$

where m_E is a constant determining Young's modulus of the soil base at a depth $z = 1$ below the surface, and B is the width of the rectangle as shown in the figures of the charts. With these influence factors the surface displacements of any point of the homogeneous or non-homogeneous half-space within or outside the loaded rectangle may readily be calculated by means of superposition. In order to be able to represent the total range of aspect ratios from the square to the strip, without loss of accuracy, in the lower range, a split-scale for the aspect ratio axis is used.

The comparison of the results for $\alpha = 0$ given in Figures 2(a)–7(a) with the solutions found by Steinbrenner[2] or Giroud[6] for the elastic half-space shows perfect agreement. For the case of a non-homogeneous base the convergence of the components u_{xx}, u_{yy}, u_{yz} and u_{zz} can be monitored for aspect ratios L/B tending to infinity and compared with the corresponding values shown in Table I and II as previously mentioned.

From Figures 2–7 it can be seen that the higher the degree of non-homogeneity gets, the more flattened the curves become and for $\alpha = 0{\cdot}9$ most of them run almost parallel to the aspect ratio axis. This indicates that with increasing non-homogeneity the influence of the aspect ratio decreases for all influence factors I_{rs} and with respect to the settlement it shows that for values of α approaching one, the settlement beneath the load becomes progressively more uniform whereas the deflection outside the loaded area becomes vanishingly small which is in accordance with

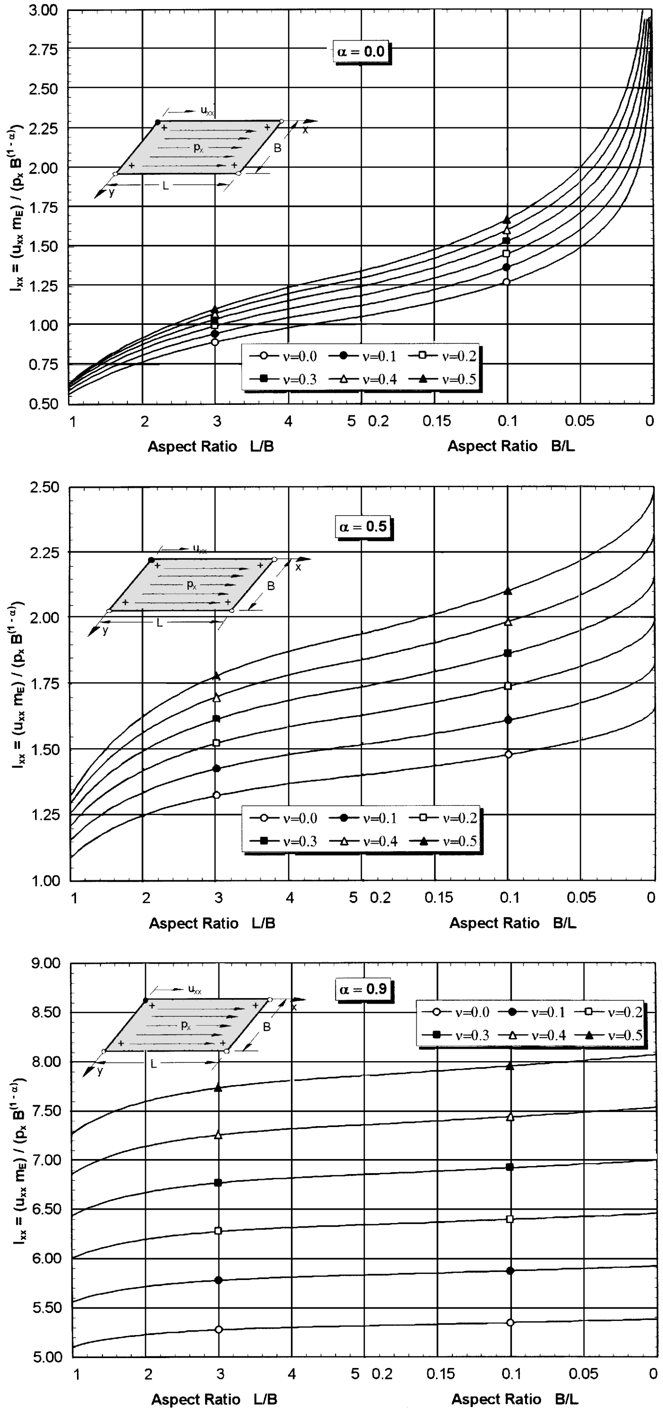

Figure 2. Influence factors for the surface displacement u_{xx} at the corner of a rectangle, due to uniform horizontal loading acting parallel to the rectangle's longer side: (a) $\alpha = 0{\cdot}0$, (b) $\alpha = 0{\cdot}5$, (c) $\alpha = 0{\cdot}9$

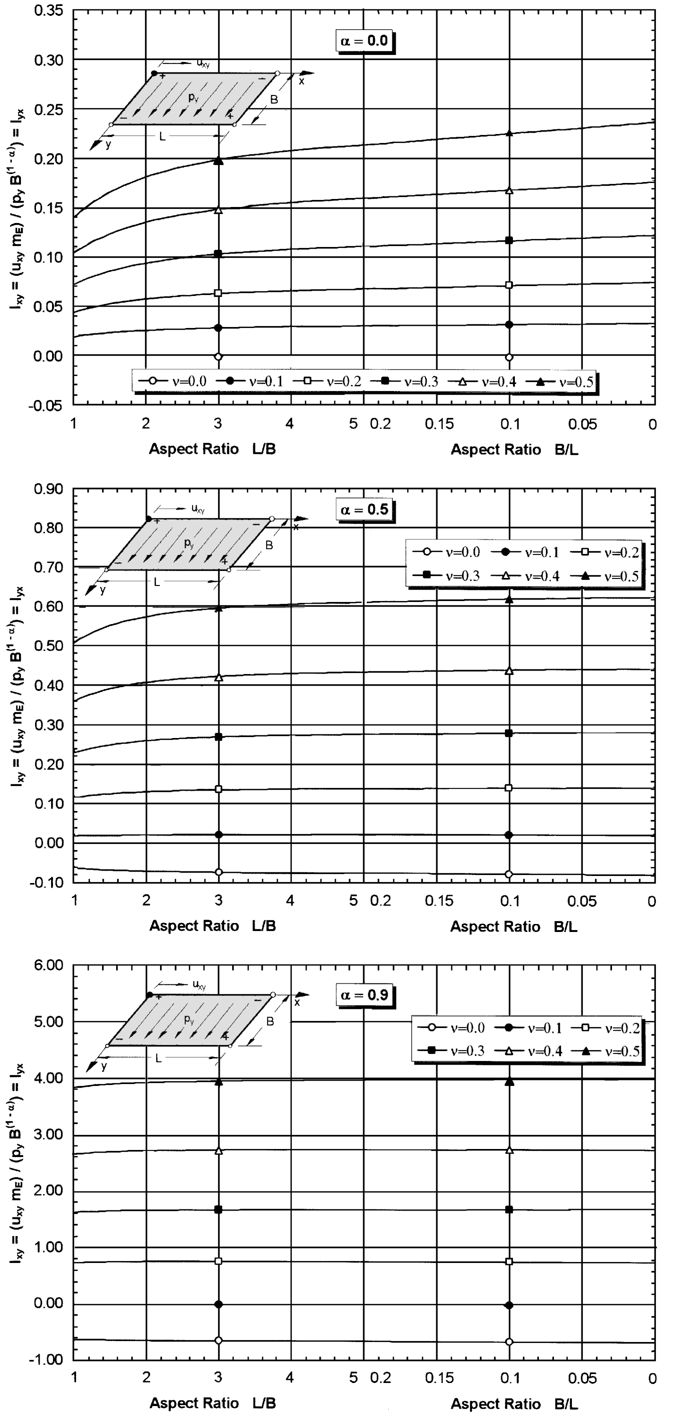

Figure 3. Influence factors for the surface displacement u_{xy} at the corner of a rectangle, due to uniform horizontal loading acting parallel to the rectangle's shorter side: (a) $\alpha = 0{\cdot}0$, (b) $\alpha = 0{\cdot}5$, (c) $\alpha = 0{\cdot}9$

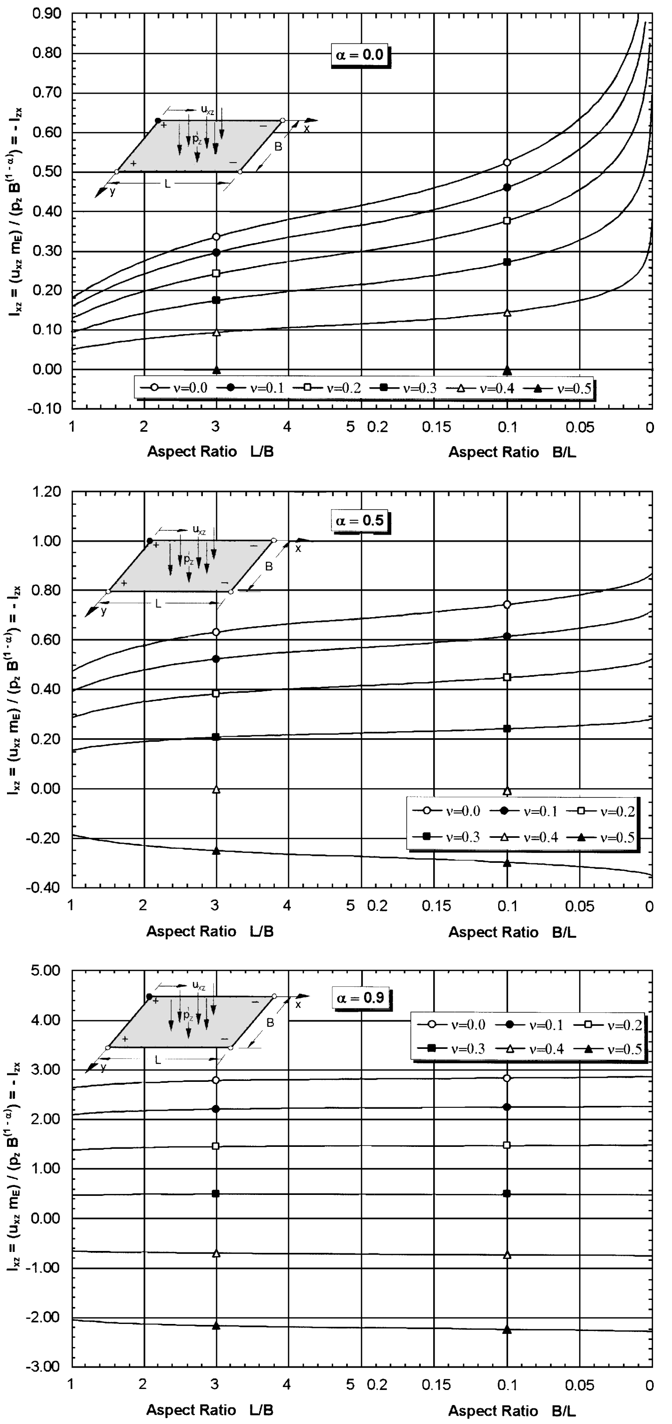

Figure 4. Influence factors for the surface displacement u_{xz} at the corner of a rectangle, due to uniform vertical loading: (a) $\alpha = 0{\cdot}0$, (b) $\alpha = 0{\cdot}5$, (c) $\alpha = 0{\cdot}9$

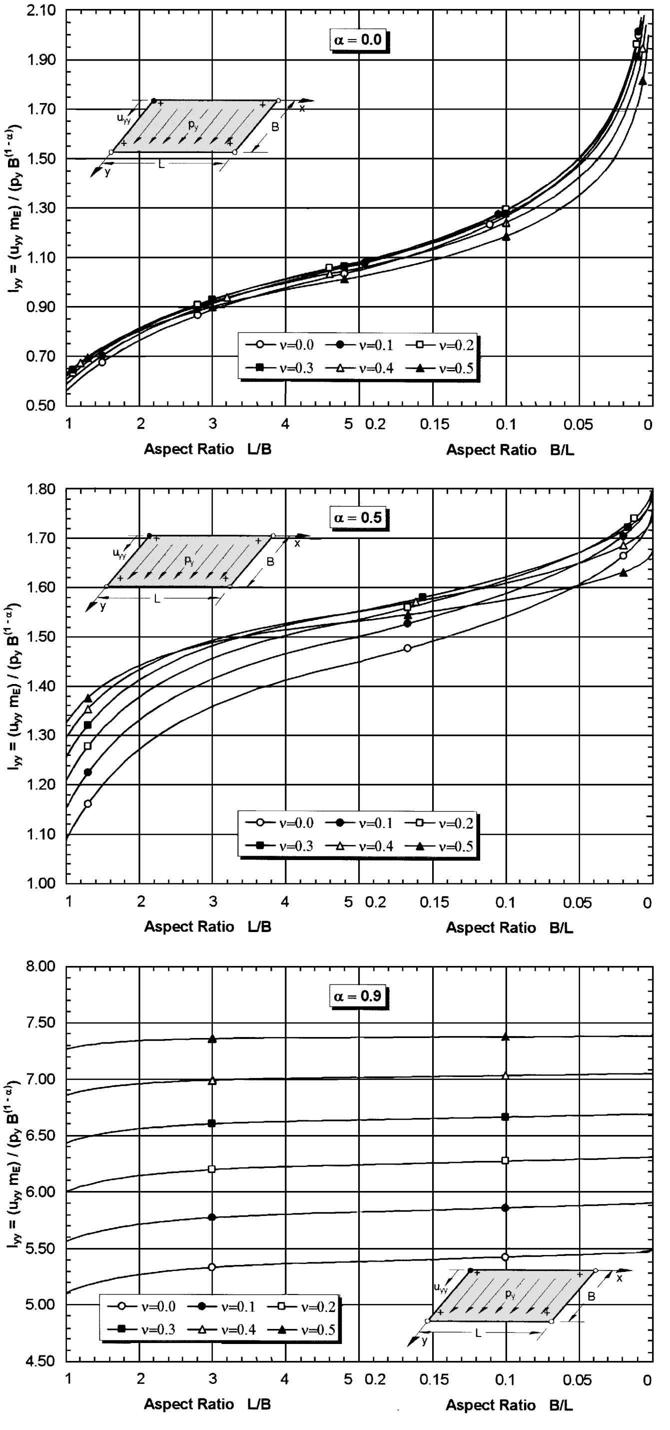

Figure 5. Influence factors for the surface displacement u_{yy} at the corner of a rectangle, due to uniform horizontal loading acting parallel to the rectangle's shorter side: (a) $\alpha = 0{\cdot}0$, (b) $\alpha = 0{\cdot}5$, (c) $\alpha = 0{\cdot}9$

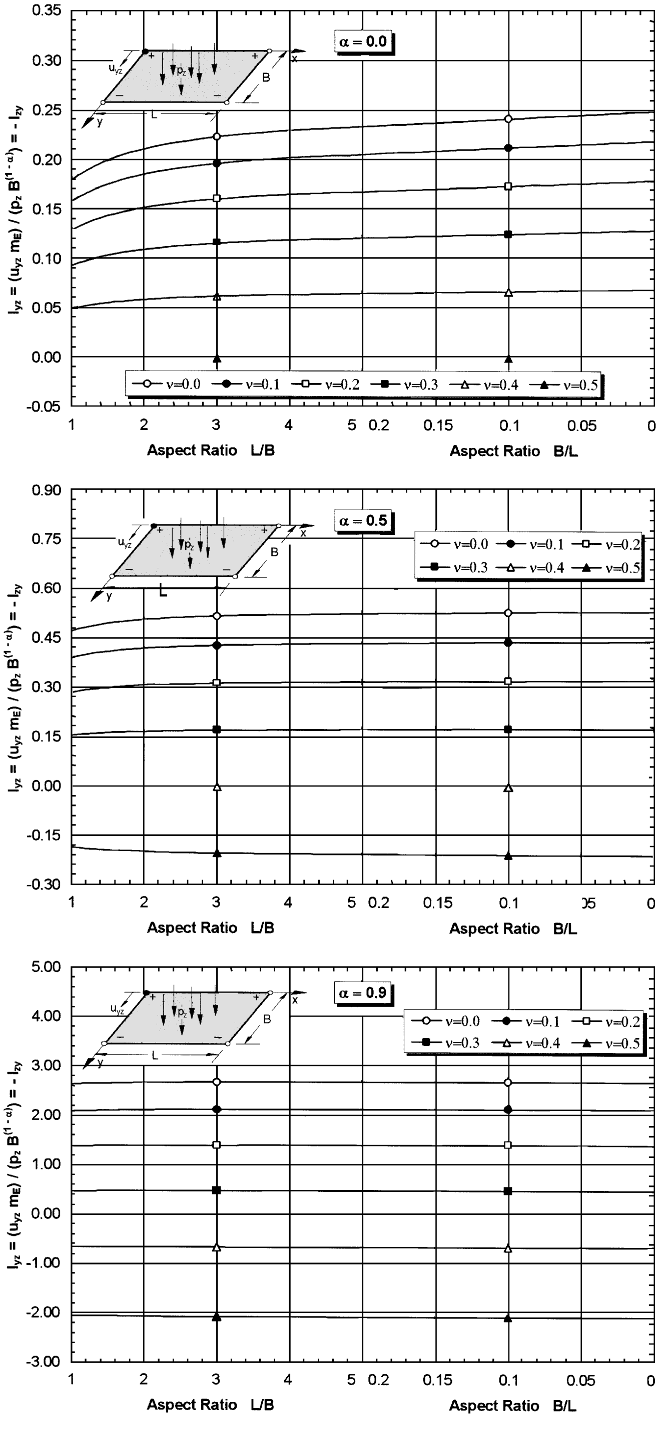

Figure 6. Influence factors for the surface displacement u_{yz} at the corner of a rectangle, due to uniform vertical loading: (a) $\alpha = 0{\cdot}0$, (b) $\alpha = 0{\cdot}5$, (c) $\alpha = 0{\cdot}9$

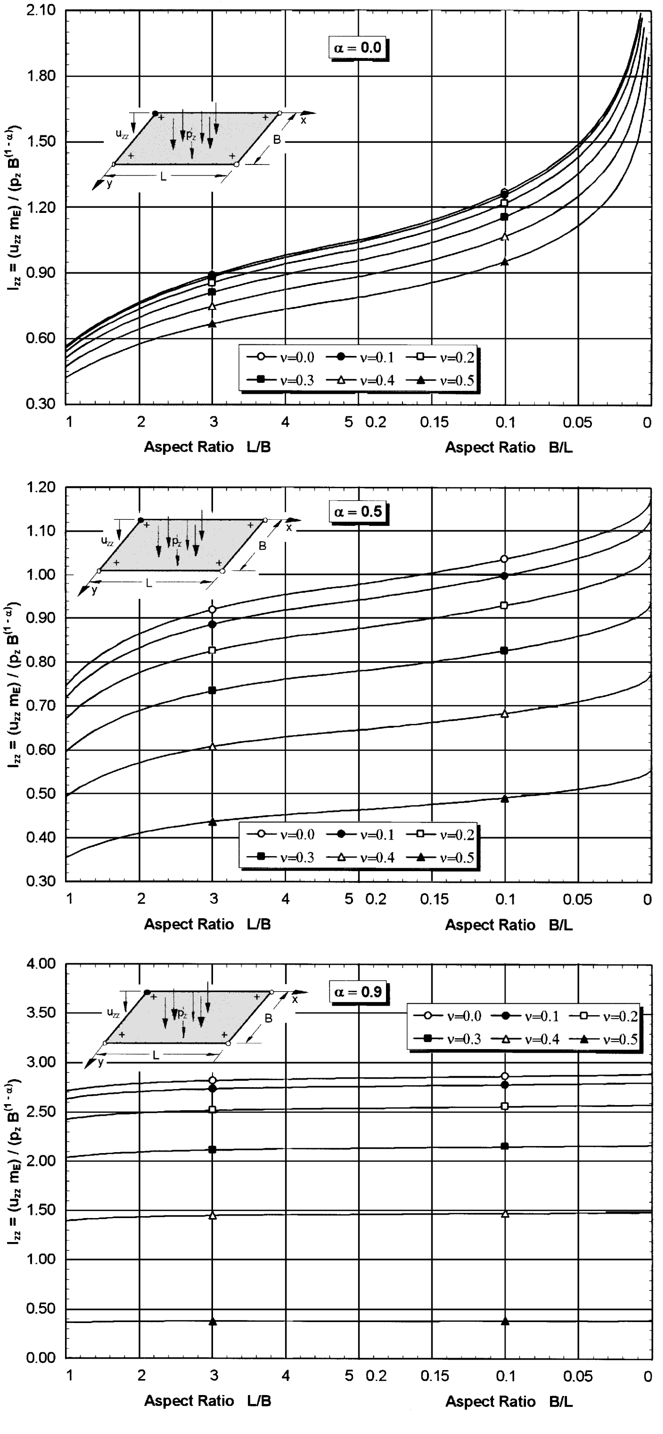

Figure 7. Influence factors for the surface displacement u_{zz} at the corner of a rectangle, due to uniform vertical loading: (a) $\alpha = 0{\cdot}0$, (b) $\alpha = 0{\cdot}5$, (c) $\alpha = 0{\cdot}9$

Gibbon's[15] results. In the limiting case of $\alpha = 1$ for all aspect ratios the settlement tends to become infinite except for an incompressible soil in which case the deflections tend to the two limiting values $3p/2m_E$ and 0 inside and outside the loaded area, respectively.

4. CONCLUSIONS

A numerical scheme has been developed to calculate the components of the surface displacements of both homogeneous and non-homogeneous half-space subject to uniformly distributed tractions on a rectangular shaped domain of the surface. The variation of Young's modulus E with depth z is assumed to have the form $E = m_E z^\alpha$ where m_E is a constant and the non-homogeneity parameter α varies between zero and unity. It was demonstrated that the surface displacement field can be found without numerical integration rendering the procedure very efficient. Numerical tests showed that the method proposed yields results which are identical with published solutions for the homogeneous half-space. For the non-homogeneous case the procedure was checked by comparing the edge displacements of a rectangle whose aspect ratio tends to infinity with well-known solutions for the strip. Again, no differences could be detected. Beyond that, comparison with the method outlined in the first part of this paper revealed identical results, proving both techniques to be working correctly. The method was then used to calculate influence charts for rectangular shaped loadings which may be used in hand calculations to estimate the surface displacements of footings on non-homogeneous soil bases. With respect to numerical applications, the procedure is well suited for use in a finite element analysis and allows taking the non-homogeneity of the base with virtually any additional computation cost into account.

ACKNOWLEDGEMENT

The work described in this paper was sponsored by the Austrian Science Foundation grant no. J0963-Tec. This support is gratefully acknowledged.

REFERENCES

1. F. Schleicher, 'Zur Theorie des Baugrundes', *Der Bauingenieur*, **7,** H. 47/48, 931, 949 (1926).
2. W. Steinbrenner, 'Tafeln zur Setzungsberechnung', *Die Straße*, **1,** 121–124 (1934).
3. F. Tölke, 'Spannungs- und Verschiebungszustände im Halbraum nach der linearen Elastizitätstheorie', *Grundbautaschenbuch*, **1,** 3. Aufl., 176–177, 182–183 (1980).
4. M. E. Harr, *Foundations of Theoretical Soil Mechanics*, McGraw-Hill, New York, 1966.
5. M. Kany, *Berechnung von Flächengründungen Band* 2, Wilhelm Ernst & Sohn, 1974.
6. J. P. Giroud, *Méchanique des sols. Tables pour la calcul des foundations*, Vols. 1 and 2, Dunod, Paris, 1972 and 1973.
7. P. T. Brown, R. E. Gibson, 'Rectangular loads on inhomogeneous elastic soil', *J. Soil Mech. Found. Div. ASCE Proc.*, **99,** No. SM10, 917–920 (1973).
8. J. R. Booker, N. P. Balaam and E. H. Davis, 'The behavior of an elastic, non-homogeneous half-space. Part I—line load and point loads', *Int. j. num. anal. Methods geomech*, **9**, 353–367 (1985a).
9. J. R. Booker, 'Analytic methods in geomechanics', in: G. Beer, J. R. Booker, J. P. Carter (eds) *Proc. 7th Int. Conf. Computer Meth. Advances Geomechanics*, Vol. 1, 3–14. 1991. pp.
10. H. G. Poulos and E. H. Davis, *Elastic Solutions for Soil and Rock Mechanics*, Wiley, New York, 1974.
11. J. R. Booker, N. P. Balaam and E. H. Davis, 'The behaviour of an elastic, non-homogeneous half-space. Part II –circular and strip footings', *Int. j. numer. anal. methods geomech.* **9,** 369–381 (1985b).
12. E. Schultze, 'Setzungen', *Grundbautaschenbuch*, **1,** 3. Aufl., 407–436 (1980).
13. J. P. Giroud, 'Settlement of a linearly loaded rectangular area', *J. Soil Mech. Found Div. ASCE*, **94,** No. SM4, 813–831 (1968).
14. R. F. Stark and J. R. Booker, 'A numerical procedure for calculating the flexibility matrix of a non-homogeneous elastic half-space subjected to uniform surface tractions. Part I—arbitrarily shaped foundations', *Research Report R698*, University of Sydney, School of Civil and Mining Engineering, 1994.
15. R. E. Gibson, 'Some results concerning displacements and stresses in a non-homogeneous elastic half-space', *Géotechnique*, **17,** 58–67 (1967).

